acta physica slovaca vol. 53 No. 1, 25 – 35 **February 2003**

RELATIVISTIC MEAN-FIELD DESCRIPTION OF Sn ISOTOPES

H. L. Yadav, U. R. Jakhar, K. C. Agarwal
Department of Physics, Rajasthan University, Jaipur 302004, India

Received 9 May 2002, in final form 19 September 2002, accepted 20 September 2002

Recently proposed BCS approach with a discretized continuum (by enclosing the nucleus in a spherical box) for the calculation of pairing energy for the drip-line nuclei within the framework of relativistic mean-field (RMF) theory is applied to the description of the ground state properties of Sn isotopes. The TMA parameter set is used for the effective mean-field Lagrangian with the nonlinear terms for the sigma and omega mesons. The results for the two neutron separation energies, and proton and neutron rms radii are shown to be in excellent agreement with the available experimental data and with the recent calculations using the relativistic Hartree-Bogoliubov (RHB) theory. Also, the calculated neutron single particle pairing gaps are found to be in agreement with the RHB and other mean-field calculations.

PACS: 21.60.Jz, 27.90.+b, 21.10.Dr, 21.10Tg

1 Introduction

The physics of exotic nuclei far from the line of β-stability constitutes one of the exciting areas of the current nuclear structure studies. As the main characteristics [1] for these nuclei, it is found that the neutron drip-line moves much farther away from the valley of β-stability, and the neutron separation energy for the last neutron is very small ($S_n < 1$ MeV) leading to a loosely bound system. Due to this weak binding and large spatial dimension of the outermost nucleons, the role of continuum states and their coupling to the bound states becomes exceedingly important, especially for the pairing energy contribution to the total binding energy of the system. Theoretical investigations for the ground state properties of such neutron rich nuclei have been carried out earlier within the frameworks of Hartree-Fock (HF) + BCS + resonant continuum [2], the Hartree-Fock-Bogoliubov (HFB) [3], and the RHB [4] theories. Also, a detailed comparative study of the HFB approach with those of the HFB based on box boundary conditions, and the HF + BCS + Resonant continuum approach mentioned above has been carried out in the context of drip line nuclei with an application to the neutron rich Ni isotopes by Grasso et al. [5].

Recently we have proposed [6] a fast BCS approach to incorporate the important contribution of single particle states to the calculation of pairing energies within the framework of relativistic mean-field (RMF) theory. In this approach the continuum is replaced by discretized positive energy states generated by enclosing the nucleus in a finite box [7]. The size of the box is chosen to be sufficiently large to enclose the nucleus and the proton and neutron density distributions

such as to provide convergence of the calculated results. From the outset it is mentioned that this procedure at best is expected to incorporate some of the main features of the continuum, especially near the Fermi surface in an approximate way. Thus the contribution to the pairing energy for a single particle sates j is obtained by solving self consistently the state dependent gap equation for the gap energy Δ_j. In our calculations we have employed a δ-function form of the pairing interaction for the sake of simplicity. It is found [6] that the resonant states which are not far away from the Fermi energy play important role and indeed contribute appreciably to the pairing energy. The pairing energy itself is known to be crucial for the description of loosely bound neutron rich systems. Indeed from the self consistent solution of the gap equation one observes that apart from the resonant states and a few of the single particle states near the Fermi surface, all other states in the continuum away from the Fermi level acquire only vary small values for the gap energy Δ_j. The validity of our present approach has been demonstrated earlier [6] by its application to the ground state properties of the entire chain of Ni isotopes.

In continuation to the above mentioned studies, we have further applied our RMF approach to investigate the ground state properties of the Sn isotopes. The results for the two neutron separation energies and the rms proton and neutron radii for the entire chain of the Sn isotopes presented here are shown to be in excellent agreement with the available experimental data and with other mean-field calculations, especially that of the RHB approach [4]. Further it is shown that the calculated neutron single particle pairing gaps for the occupied states, and the neutron density profiles from our RMF calculations have values similar to those obtained in the RHB calculations [4] using the NL3 effective mean-field Lagrangian whereby the pairing correlations are described by the pairing part of the finite range Gogny interaction. Our conclusions in fact are very much in line with the recent results of Grasso et al. [5] wherein it has been shown that the BCS approach provides a good approximation to the more complete Bogoliubov calculations even near the drip lines. Extending this result of ref. [5] to the relativistic approach, it is reasonable to infer that the RMF + BCS results are likely to be close to those of the RHB calculations [4].

2 Theoretical Formulation and Model

Our RMF calculations have been carried out using the model Lagrangian density [8–13] with nonlinear terms both for the σ and ω mesons, and is given by [13]

$$\begin{aligned}
\mathcal{L} &= \bar{\Psi}[\imath\gamma^{\mu}\partial_{\mu} - M]\Psi \\
&+\frac{1}{2}\,\partial_{\mu}\sigma\partial^{\mu}\sigma - \frac{1}{2}m_{\sigma}^{2}\sigma^{2} - \frac{1}{3}g_{2}\sigma^{3} - \frac{1}{4}g_{3}\sigma^{4} - g_{\sigma}\bar{\Psi}\sigma\Psi \\
&-\frac{1}{4}H_{\mu\nu}H^{\mu\nu} + \frac{1}{2}m_{\omega}^{2}\omega_{\mu}\omega^{\mu} + \frac{1}{4}c_{3}(\omega_{\mu}\omega^{\mu})^{2} - g_{\omega}\bar{\Psi}\gamma^{\mu}\Psi\omega_{\mu} \\
&-\frac{1}{4}G_{\mu\nu}^{a}G^{a\mu\nu} + \frac{1}{2}m_{\rho}^{2}\rho_{\mu}^{a}\rho^{a\mu} - g_{\rho}\bar{\Psi}\gamma_{\mu}\tau^{a}\Psi\rho^{\mu a} \\
&-\frac{1}{4}F_{\mu\nu}^{a}F^{a\mu\nu} - e\bar{\Psi}\gamma_{\mu}\frac{(1-\tau_{3})}{2}A^{\mu}\Psi\ ,
\end{aligned}$$

where the field tensors, H, G and F for the vector fields are defined through

$$H_{\mu\nu} = \partial_{\mu}\omega_{\nu} - \partial_{\nu}\omega_{\mu}$$

$$\begin{aligned} G^a_{\mu\nu} &= \partial_\mu \rho^a_\nu - \partial_\nu \rho^a_\mu - g_\rho\, \epsilon^{abc} \rho^b_\mu \rho^c_\nu \\ F_{\mu\nu} &= \partial_\mu A_\nu - \partial_\nu A_\mu \ . \end{aligned} \tag{1}$$

The symbols M, m_σ, m_ω, and m_ρ, are the mass of nucleon, and that of the σ, ω, and ρ mesons, respectively. Similarly, g_σ, g_ω, g_ρ and $e^2/4\pi = 1/137$ are the coupling constants for the different mesons, and the photon, respectively. For the σ meson in the Lagrangian density (1), the nonlinear potential is assumed to have the form [12]

$$U(\sigma) = \frac{1}{2} m_\sigma \sigma^2 + \frac{1}{3} g_2 \sigma^3 + \frac{1}{4} g_3 \sigma^4 \,, \tag{2}$$

where g_2 and g_3 are the self coupling constants. The self coupling term for the ω meson introduced in ref. [13] has a quartic form and is given by

$$V(\omega) = \frac{1}{4} c_3 (\omega_\mu \omega^\mu)^2 \,. \tag{3}$$

Introduction of such a nonlinear coupling term has been shown to yield a vector potential having main features similar to that of the vector potential obtained [14] in a relativistic Brueckner-Hartree-Fock (RBHF) description. In the present treatment we restrict our studies to the case of spherical mean fields. In this case the wave function for the nucleon can be written as [15]

$$\psi_\alpha = \frac{1}{r} \begin{pmatrix} i\ G_\alpha\ \mathcal{Y}_{j_\alpha l_\alpha m_\alpha} \\ F_\alpha\ \frac{\sigma \cdot p}{r}\ \mathcal{Y}_{j_\alpha l_\alpha m_\alpha} \end{pmatrix} \,, \tag{4}$$

where the normalization condition is given by

$$\int dr \, \{ |G_\alpha|^2 \, + \, |F_\alpha|^2 \} \, = \, 1 \,. \tag{5}$$

Here G_α and F_α denote the radial wave functions for the upper and lower components, respectively, and the symbol $\mathcal{Y}_{j_\alpha l_\alpha m_\alpha}$ has been used for the spinor spherical harmonics. With this wave function, the final expressions for the various densities are simplified and can be written in a compact form [8]. Similarly, one obtains simple coupled equations for the nuclear radial wave functions F_α and G_α amenable easily to numerical evaluations [8].

The set of parameters appearing in the effective Lagrangian (1) have been obtained in an extensive study [13] which provides a reasonably good description for the ground state of nuclei and that of the nuclear matter properties. This set, termed as TMA [13], has an A-dependence and covers the light as well as medium heavy nuclei from ^{16}O to ^{208}Pb. The parameter values are as given below. The mass of nucleon, and that of sigma, omega and rho mesons are, respectively, $M = 938.9$ MeV, $m_\sigma = 519.151$ MeV, $m_\omega = 781.950$ MeV, $m_\rho = 768.100$ MeV. The effective strengths of the coupling between various mesons and nucleons have values $g_\sigma = 10.055 + 3.050/A^{0.4}$, $g_\omega = 12.842 + 4.644/A^{0.4}$, $g_\rho = 3.800 + 4.644/A^{0.4}$. The nonlinear coupling strengths of the sigma meson are given by $g_2 = -0.328 - 27.879/A^{0.4}$ fm^{-1}, and $g_3 = 38.862 - 184.191/A^{0.4}$, whereas the self coupling of the omega field has the strength $c_3 = 151.590 - 378.004/A^{0.4}$. As mentioned above, we have used the δ-function force, $V = -V_0\, \delta(r)$ for the calculation of pairing energy within the BCS approach. The value of the interaction strength $V_0 = 350$ MeV·fm^3 was determined in ref. [6] by obtaining a best fit to the binding energy of Ni isotopes. We use the same vale of $V_0 = 350$ MeV·fm^3, for our present

studies of Sn isotopes as well. Apart from its simplicity, the applicability and justification of using such a δ-function form of interaction has been recently discussed in ref. [3, 7] whereby it has been shown in the context of HFB calculations that the use of a delta force in a finite space simulates the effect of finite range interaction in a phenomenological manner (see also [16] and [17] for more details).

The BCS solution [18, 19] for the gap parameter Δ_j for a given state has the form

$$\Delta_{j_1} \;=\; -\frac{1}{2}\frac{1}{\sqrt{2j_1+1}}\sum_{j_2}\frac{\left\langle (j_1{}^2)\,0^+\,|V|\,(j_2{}^2)\,0^+\right\rangle}{\sqrt{\left(\varepsilon_{j_2}\,-\,\lambda\right)^2\,+\,\Delta_{j_2}^2}}\;\sqrt{2j_2+1}\;\;\Delta_{j_2}\;, \tag{6}$$

where ε_{j_2} are the single particle energies, and λ is the Fermi energy; whereas the particle number condition is given by $2\sum_{j>0}\,v_j^2\;=\;N$. Further, the pairing matrix element for the δ-function force is given by

$$\left\langle (j_1{}^2)\,0^+\,|V|\,(j_2{}^2)\,0^+\right\rangle \;=\; \frac{V_0}{8\pi}(-1)^{l_1+l_2}\;\sqrt{(2j_1+1)(2j_2+1)}\;\,I_R\;, \tag{7}$$

where I_R is the radial integral having the form

$$I_R \;=\; \int dr\frac{1}{r^2}\,\left(G_{j_1}^{\star}\,G_{j_2}\,+\,F_{j_1}^{\star}\,F_{j_2}\right)^2\,. \tag{8}$$

From the form of eqs. (7) and (8) it is clearly seen that the contribution to the pairing gap is significant only from those positive energy states which have sizable overlap with the bound single particle states near the Fermi surface. The resonant states having the characteristic of being confined within the range of the mean field potential, similar to the bound states, thus have maximum contributions.

As mentioned above, the coupled field equations obtained from the Lagrangian density in (1) are finally reduced [8] to a set of simple radial equations which are solved self consistently along with the equations for the state dependent pairing gap Δ_j and the total particle number N for a given nucleus. In what follows we discuss the details of our calculations and results for ^{150}Sn nucleus which is treated as a representative case of our studies for the entire chain of isotopes. In our calculations the spacing in the grid for the r-space is taken to be 0.1 fm, and the maximum radial distance $R_{\max}$ is chosen to be several times that of the nuclear radius such as to yield convergence for the calculated ground state properties of the nucleus under consideration. In the present studies of Sn isotopes, for example, a value of $R_{\max}$ = 30 fm is found to be sufficient for the convergence of the results. Similar studies have been carried out to check the stability of results with respect to the number of states available for the description of the positive energy states.

3 Results and Discussion

In order to describe the contribution of various single particle states to the pairing energy, we plot in Fig. 1 the calculated pairing gap energies of the neutron single particle states near the Fermi surface for the nucleus ^{150}Sn. The figure also shows the resonant $1i_{13/2}$ state at 0.35 MeV. There are many non-resonant states in the positive energy side of the figure, but these are not

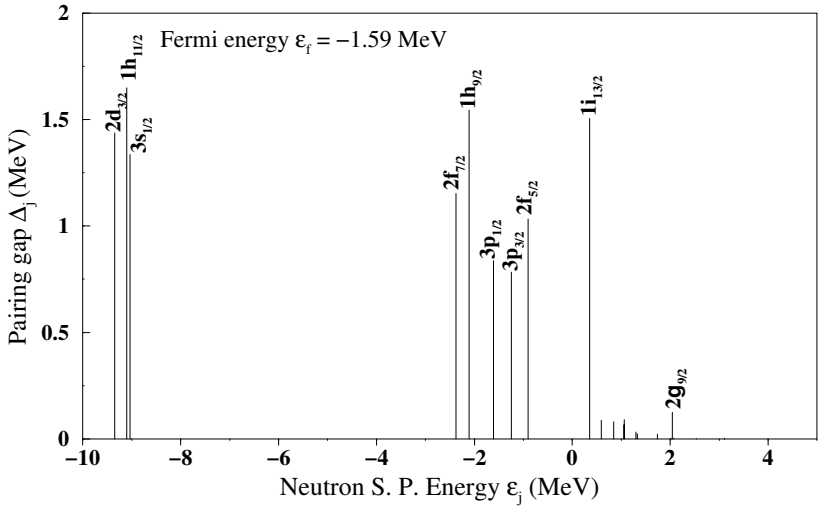

Fig. 1. The pairing gap energy Δ_j for the neutron single particle states near the Fermi surface for the nucleus ^{150}Sn. The resonant $1i_{13/2}$ state at 0.35 MeV is seen to have large pairing gap similar to the bound single particle states.

shown here. The formation of resonant states can be simply understood in terms of transmission of waves passing through an attractive potential well augmented with a centrifugal potential barrier. The effective total potential has an appreciable barrier for the trapping of waves to form a resonant state. Such a metastable state remains mainly confined to the region of the potential well and the wave function exhibits characteristics similar to that of a bound state. This is clearly seen in Fig. 2 which shows the radial wave functions of some of the neutron single particle states lying close to the Fermi surface, the neutron Fermi energy being $\lambda_n = -1.59$ MeV. These include the bound $2f_{5/2}$ and $1h_{9/2}$, and the continuum single particle states, $1i_{13/2}$, $4s_{1/2}$ and $1i_{11/2}$. The wave function for the $1i_{13/2}$ state is clearly seen to be confined within a radial range of about 10 fm and has only a decaying component outside this region, characterizing a resonant state. In contrast the main part of the wave function for non-resonant state $1i_{11/2}$ is seen to be spread over mostly outside the potential region. This state thus has a negligible overlap with the bound states near the Fermi surface leading to almost zero value for the pairing gap $\Delta_{1i_{11/2}}$. Such non-resonant states thus do not contribute to the total pairing energy for the system. The next important states are the loosely bound states. A representative example of such a state is the $2f_{5/2}$ state at -0.90 MeV. From Fig. 2 it is seen that this state has a sizable part of the wave function within the region of the potential well and thus provides rather significant contribution to the pairing energy.

In view of the fact that the RHB calculations [4] are considered to represent the most reliable treatment presently available for the weakly bound system, a comparison of our RMF neutron single particle pairing gap energy Δ_j with those obtained in the RHB calculations [4] is expected to shed light on the validity of our calculations for the treatment of drip-line nuclei. It is found that our Δ_j values for the occupied states ranging between 1 MeV to 1.9 MeV are similar to

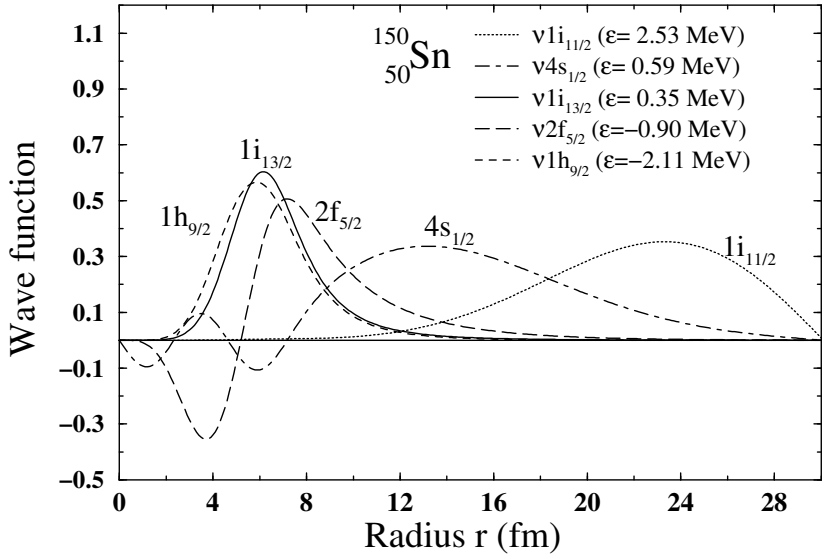

Fig. 2. Radial wave function of a few representative neutron single particle states with energy close to the Fermi surface for the nucleus ^{150}Sn. The solid line shows the resonant $1i_{13/2}$ state at energy 0.35 MeV which is confined within the potential region similar to the bound $1h_{9/2}$ state at -2.11 MeV shown by dashed line.

the results of HFB and RHB calculations [3, 4]. The RHB calculations [4] with the Gogny force for the pairing correlations yield values which lie between about 1.5 MeV to 2.7 MeV, whereas the HFB results [3] range from about 0.5 MeV to 1.75 MeV for the SKP (Skyrme-pairing force) interaction and from 1.25 MeV to 1.50 MeV for the SKP$^{\delta}$ (Skyrme-pairing force, with a surface peaked delta interaction for pairing) interaction. The total average neutron pairing energy for the Sn isotopes follows the inverse parabolic shape with vanishing values at the neutron number $N = 50,\ 82$ and 126. This agreement of our RMF results with those of RHB and HFB calculations for the pairing correlations characteristic is very gratifying and provides strong support to our BCS approach for the weakly bound systems.

It is emphasized that the position and the gap energy of a resonant state, like that of $1i_{13/2}$, do not change with the increase in the value of $R_{\max}$ used for the RMF calculations after a $R_{\max}$ for the convergent solution has been fixed. In contrast it is usually not true for the non-resonant continuum states. However, this change in position and occupation probabilities of the continuum states does not effect the final results of total binding energy, average pairing gap energy and the values of various rms radii.

Another important aspect of the neutron rich nuclei is the formation of defused neutron skin [1]. For the nucleus ^{150}Sn this characteristic feature is demonstrably seen in Fig. 3 wherein we plot the density distribution of protons for the nucleus ^{172}Sn by hatched lines and that of the neutrons for three different isotopes ^{118,150,172}Sn by solid lines. The tail of the neutron density in the ^{150,172}Sn isotopes extends far beyond the mean field potential and has appreciable value up

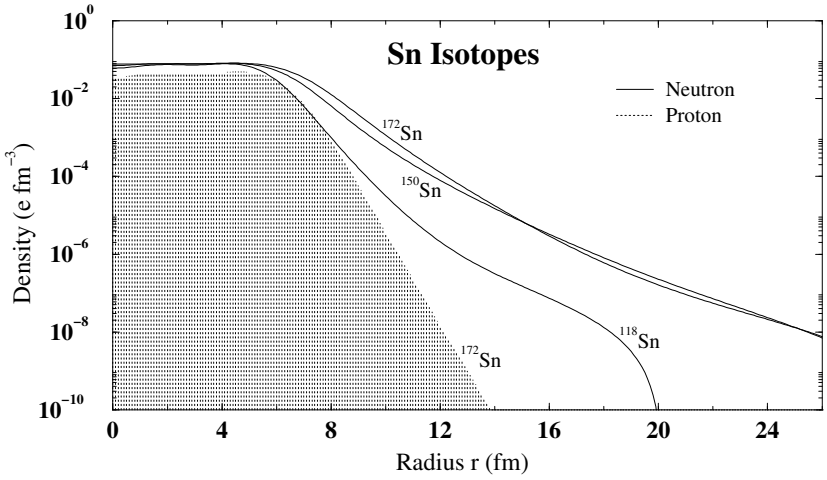

Fig. 3. The neutron radial density distribution obtained for the ^{118,150,172}Sn isotopes have been shown by solid lines. The hatched area represents the proton radial density distribution for the nucleus ^{172}Sn.

to about 15 fm. The proton densities are almost similar for different isotopes and we have shown only the results for the nucleus ^{172}Sn. The sharp fall off of the proton density distribution within a smaller distance as compared to that of neutron density is expected since the number of protons is small and the binding energy is large. Further it is found that our RMF results for the density distributions are in good agreement with the RHB calculations [4] (as can be seen from Fig. 4 of [4]). A study of the neutron density profile reveals information about nature of the surface thickness and diffuseness parameter. The surface thickness t is defined as the required change in radius to reduce $\rho(r)/\rho_0$ from 0.9 to 0.1 where ρ_0 is the maximum value of the neutron density. The diffuseness parameter α is determined by fitting the neutron density profiles to the Fermi distribution. It is found that with additional number of neutrons the surface thickness increases uniformly from about 1.75 fm in ^{100}Sn to about 3.4 fm in ^{176}Sn. Similar increase of about 90% is found for the diffuseness parameter α.

In Fig. 4 we plot the results of two neutron separation energy for the entire chain of Sn isotopes covering the proton and neutron drip-lines. The figure also shows the RHB calculations of ref. [4], along with the experimental data available [20] for the $^{98-136}$Sn isotopes for the purpose of comparison. It is to be noted that in the figure the experimental data shown by solid circles have been distinguished by the extrapolated data shown by open squares. It is gratifying to note that our RMF results are in excellent agreement with the data. The strong variations in the experimental separation energy near the neutron magic numbers $N = 50$, and 82 are well accounted for by our calculations. The overall agreement with the RHB calculations [4] is also readily seen.

Another interesting result is the prediction of the two neutron drip-line. In our calculations it is found to occur at $A = 176$ $(N = 126)$ which is in accord with that of the HFB and RHB calculations [3, 4]. Similarly our calculations show that the proton drip-line occurs at $A = 96$ $(N = 46)$. For this purpose calculations for the fixed value of $N = 46$ were carried out for the

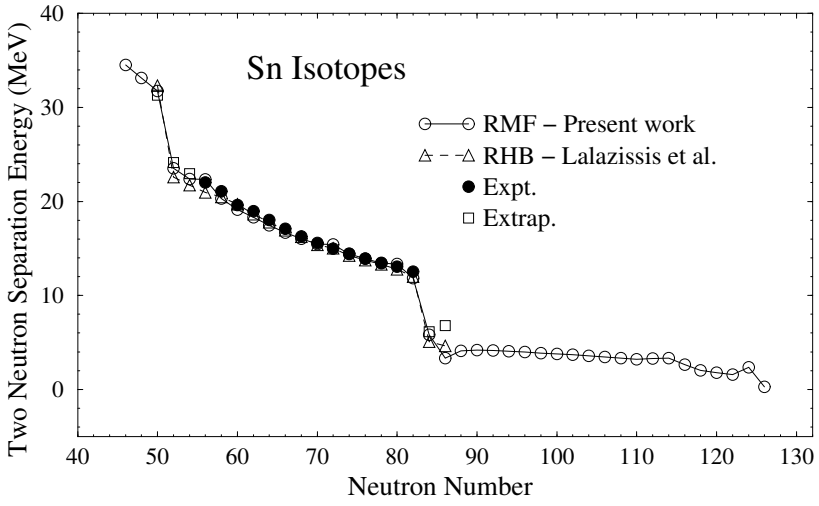

Fig. 4. The present RMF results for the two neutron separation energy as a function of neutron number for the $^{96-176}$Sn isotopes shown by open circles are compared with the available experimental data [20] for $^{50-136}$Sn isotopes depicted by solid circles. Open squares represent the extrapolated experimental data in ref. [20]. The results of RHB theory [4] have been shown by open triangles.

neighboring nuclei with atomic number $Z = 46$, 48, 50, 52. The results show that ^{96}Sn is the most bound system (B.E. = 765.9103 MeV). The nucleus ^{98}Te is unbound with its last two proton in the continuum. The nucleus ^{94}Cd is found to be bound with B.E. = 764.6087 MeV. Similarly the nucleus ^{92}Pd has a binding energy of 761.7119 MeV. Thus the two proton separation energy between ^{96}Sn and ^{94}Cd is about 1.3 MeV. From this we conclude that the two proton drip line is represented by the isotope ^{96}Sn with $N = 46$.

The stability of such extremely neutron rich nuclei can be understood by studying the detailed single particle spectra and the variation of the Fermi energy with the addition of neutrons. Indeed it is found that the $1i_{13/2}$ state plays a crucial role in the sense that up to the neutron number $N = 112$, it adds to the binding through its contribution to the pairing energy by being a resonant state. Beyond the neutron number $N = 112$ this state becomes a bound one and contributes to the stability of neutron rich nucleus by accommodating more neutrons until it is completely filled at $N = 126$. Further addition of two neutrons fills the $4s_{1/2}$ level having energy 250 keV, which lies in the continuum. The total binding energy of the isotope ^{178}Sn is less than that of ^{176}Sn by about 497 keV and thus the nucleus corresponding to $N = 126$ is suggested to be the heaviest stable isotope. It is found that the RMF theory yields a weaker spin orbit interaction with the addition of neutrons. Consequently the energy splitting between the spin-orbit partners, for example, $1h_{11/2}$ and $1h_{9/2}$ states, is gradually reduced from 8.2 MeV in ^{100}Sn to 5.9 MeV in ^{150}Sn, and gets further reduced to 5.1 MeV in ^{172}Sn as more and more neutrons are added to the system. This finding is in accord with the RHB results of Lalazissis et al. [4]. Further, we observe that this change in the nature of the spin-orbit interaction for very rich neutron isotopes

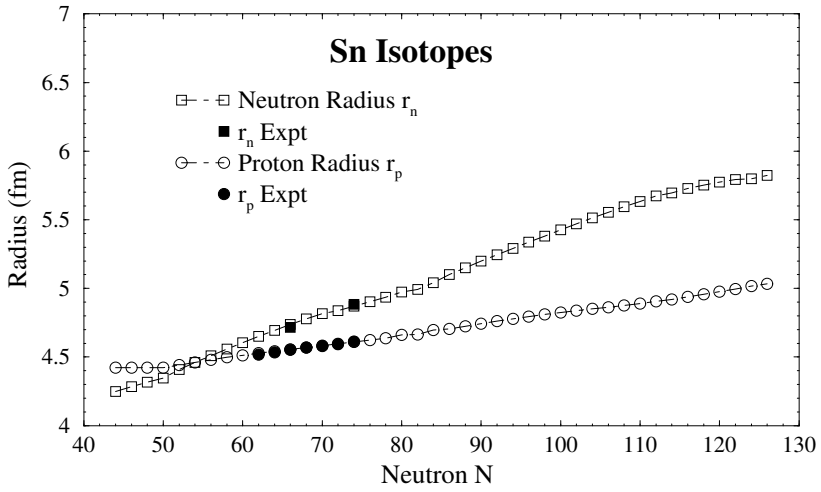

Fig. 5. Calculated neutron and proton radii as a function of neutron number for various Sn isotopes shown by open squares and circles are compared with the available experimental data [21, 22] depicted by solid squares and circles, respectively.

results in a negligible energy splitting of other high lying high angular momentum states. For example the $1i_{11/2}$ and $1i_{13/2}$ spin-orbit partners usually have energy splitting of several MeV and this results in the neutron and proton magic numbers. In contrast for extremely neutron rich nuclei, for example in the case of $^{150,172}\mathrm{Sn}$ nuclei this splitting is only about 2 to 4 MeV for these two states. We looked for additional high lying resonant states apart from the $i_{13/2}$ state. Another resonant state, in particular a resonant $j_{15/2}$ state within a few MeV (larger than the average gap energy) above the $1i_{13/2}$ state was not found. Such states if found far away from the Fermi level, as such do not contribute significantly. From the figure it is observed that the change in separation energy is almost gradual for all the isotopes except at the magic numbers 50, 82 and 126. Between $N = 84$ to $N = 124$ it is almost constant with small variation and gets abruptly reduced to a small value of 0.29 MeV for $N = 126$ which corresponds to the nucleus $^{176}\mathrm{Sn}$. Very neutron rich isotopes having small separation energies of the order of a few MeV ($\approx$ 2–4 MeV) represent loosely bound system.

In contrast to the binding energy, the experimental data on the proton and neutron root mean square (rms) radii are available only for a few of the Sn isotopes [21,22]. The measured values for the proton rms radii [21] of $^{112-124}\mathrm{Sn}$ and that for the neutron rms radii [22] of $^{116,124}\mathrm{Sn}$ isotopes are found to be in excellent agreement with our calculations as seen from Fig. 5. Our results once again are seen to compare well with that of the RHB calculations reported in ref. [4]. The RMF calculations predict a uniform increase of rms radii with the neutron number N. However, it does not follow exactly the $N^{1/3}$ systematics for the entire chain of isotopes, especially for the drip-line nuclei. At the same time the calculations do not show any abrupt increase in the neutron rms radius as well. The neutron skin $\mathrm{r_n} - \mathrm{r_p}$ increases from -0.08 fm for $^{100}\mathrm{Sn}$ to 0.33 fm for $^{132}\mathrm{Sn}$, and then further to 0.78 fm for $^{176}\mathrm{Sn}$ isotope. For the neutron rich isotopes near the drip line the

variation in neutron rms radius can be understood in terms of the occupancy of levels viz., the $1i_{13/2}$ and $4s_{1/2}$ close to the Fermi surface. In contrast to the bound $1i_{13/2}$ state, the $4s_{1/2}$ state being in the continuum does not have appreciable localization inside the nucleus. Therefore, the contribution to the neutron rms radius from the $4s_{1/2}$ state is expected to be more than that from the $1i_{13/2}$ state assuming that both have the same occupancy. For $A > 156$ the occupancy of the bound $1i_{13/2}$ state increases steadily as we add more neutrons. On the other hand the $4s_{1/2}$ state continues to be in the continuum just above the Fermi level and its very small occupancy does not change appreciably. This is the reason that we do not see pronounced rapid increase in the neutron rms radius and there is no obvious indication for the formation of neutron halo [23, 24] as we reach the neutron drip line.

4 Conclusions

To summaries, we have applied the BCS approach using a discretized continuum within the framework of relativistic mean-field theory to study the ground state properties of Sn isotopes up to the drip-lines. The TMA set parameter has been used for the effective mean-field Lagrangian which contains a nonlinear term for the ω meson in addition to the usual nonlinear terms for the σ meson. For the pairing calculation we have employed the δ-function interaction. Out of many positive energy states, the resonant states are found to play important role, especially for the neutron rich nuclei with small two neutron separation energy. The resonant states are found to have gap energy Δ_j as large as those of the bound states. This has been demonstrated by our calculations for the $^{150}\mathrm{Sn}$ isotope in detail. Our calculated results for the two neutron separation energy, rms neutron and proton radii and the pairing gap energies compare well with the known experimental data and with other state of the art calculations like that of the RHB [4]. This conclusion is in accord with the recent illuminating study of Grasso et al. [5] whereby the BCS approach is shown to be a good approximation to the more complete Bogoliubov treatment even for nuclei close to the drip lines. Finally, Our calculations show that the two neutron drip line nucleus for the Sn isotopes is $^{176}\mathrm{Sn}$, whereas the two proton drip line is represented by $^{96}\mathrm{Sn}$.

Acknowledgement: The subject of present work was initiated during one of the authors (HLY) stay at RCNP, Osaka University, Osaka. He would like to thank Prof. H. Toki and Dr. S. Sugimoto for numerous fruitful discussions. He also acknowledges financial support under the project no. SP/S2/K-28/97 by the Department of Science and Technology (DST), India.

References

[1] I. Tanihata: *J. of Phys.* **G 22** (1996) 157

[2] N. Sandulescu, Nguyen Van Giai, R. J. Liotta: *Phys. Rev.* **C 61** (2000) 061301(R)

[3] J. Dobaczewski, W. Nazarewicz, T. R. Werner, J. F. Berger, C. R. Chinn, J. Decharge: *Phys. Rev.* **C 53** (1996) 2809

[4] G. A. Lalazissis, D. Vretenar, P. Ring: *Phys. Rev.* **C 57** (1998) 2294

[5] M. Grasso, N. Sandulescu, N. Van Giai, R. J. Liotta: *Phys. Rev.* **C 64** (2001) 064321

[6] H. L. Yadav, S. Sugimoto, H. Toki: To be published, Preprint, RCNP, Osaka University, Osaka (2001); H. Toki, N. Sandulescu, J. Meng, H. L. Yadav, S. Sugimoto: Contribution to the JPS Spring Meeting, 2002

[7] J. Dobaczewski, H. Flocard, J. Treiner: *Nucl. Phys.* **A 422** (1984) 103;
J. Terasaki, P.-H. Heenen, H. Flocard, P. Bonche: *Nucl. Phys.* **A 600** (1996) 371

[8] P. G. Reinhard, M. Rufa, J. Marhun, W. Greiner, J. Friedrich: *Z. Phys.* **A 323** (1986) 13;
P. G. Reinhard: *Rep. Prog. Phys.* **52** (1989) 439 and references therein

[9] Y. K. Gambhir, P. Ring, A. Thimet: *Ann. Phys.* **198** (1990) 132;
P. Ring: *Prog. Part. Nucl. Phys.* **37** (1996) 193 and references therein

[10] J. D. Walecka: *Ann. Phys. (NY)* **83** (1974) 491

[11] B. D. Serot, J. D. Walecka: *Adv. Nucl. Phys.* **16** (1986) 1 and references therein

[12] J. Boguta, A. R. Bodmer: *Nucl. Phys.* **A 292** (1977) 413

[13] Y. Sugahara, H. Toki: *Nucl. Phys.* **A 579** (1994) 557

[14] R. Brockman, H. Toki: *Phys. Rev. Lett.* **68** (1992) 3408

[15] J. D. Bjorken, S. D. Drell: *Relativistic Quantum Mechanics*, Mc Graw Hill, New York (1964)

[16] G. F. Bertsch, H. Esbensen: *Ann. Phys. (N.Y.)* **209** (1991) 327

[17] A. B. Migdal: *Theory of Finite Fermi Systems and Applications to Atomic Nuclei*, Interscience, New York (1967)

[18] A. M. Lane: *Nuclear Theory*, Benjamin, New York (1964)

[19] P. Ring, P. Schuck: *The Nuclear many-body Problem*, Springer, Berlin (1980)

[20] G. Audi, A. H. Wapstra: *Nucl. Phys.* **A 595** (1995) 409

[21] H. de Vries, C. W. de Jager, C. de Vries: *At. Data Nucl. Data Tables* **36** (1987) 495

[22] C. J. Batty, E. Friedman, H. J. Gils, H. Rebel: *Adv. Nucl. Phys.* **19** (1989) 1

[23] S. Mizutori, J. Dobaczewski, G.A. Lalazissis, W. Nazarewicz, P. G. Reinhard: *Phys. Rev.* **C 61** (2000) 044326

[24] A. S. Jensen, K. Riisager: *Phys. Lett.* **B 480** (2000) 39